Title
ELECTRON LOADING AND HIGH VOLTAGE SPARKING OF METALS IN VACUUM

Author
Heard, Harry G.

Publication Date
1953-06-29

UNIVERSITY OF CALIFORNIA

Ernest O. Lawrence

Radiation Laboratory

BERKELEY, CALIFORNIA

DISCLAIMER

UCRL-2252
Unclassified - Physics Distribution

cy 2.

UNIVERSITY OF CALIFORNIA

Radiation Laboratory

Contract No. W-7405-eng-48

ELECTRON LOADING AND HIGH VOLTAGE SPARKING OF METALS IN VACUUM

Harry G. Heard

June 29, 1953

Berkeley, California

ELECTRON LOADING AND HIGH VOLTAGE SPARKING OF METALS IN VACUUM

Harry G. Heard

Radiation Laboratory, Department of Physics
University of California, Berkeley, California

June 29, 1953

ABSTRACT

Statistical methods were employed to measure relative values of electron loading and spark-over voltage for a large number of unoutgassed electrode materials. Test voltages up to 110 KV were employed in vacuum of the order of 10^{-7} mm Hg.

All metals showed a square-root dependence between spark-over voltage and spacing. Electron loading as well as spark-over voltage are shown to be dependent on electrode gap shunt capacity. Electron loading was an exponential function of the applied field. The constants for these empirical relations are given for fixed experimental conditions. Metals are classified separately as to electron loading and voltage holding capacity.

Unclassified - Physics Distribution

ELECTRON LOADING AND HIGH VOLTAGE SPARKING OF METALS IN VACUUM

Harry G. Heard

Radiation Laboratory, Department of Physics
University of California, Berkeley, California

June 29, 1953

INTRODUCTION

Electrons may be obtained from metals under widely varying experimental conditions. When based on the Fermi-Sommerfeld picture of a metal, the electron current density can be expressed approximately as[1]

$$J \cong \int_{W_a}^{\infty} N(W)P(W,\nu)D(W,E)dW$$

or

$$J \cong \int_{0}^{\infty} N(\epsilon)P(\epsilon,\nu)D(\epsilon,E)d\epsilon \qquad (1)$$

where W is the energy corresponding to the velocity component of the electron normal to the metal before it absorbs a photon; $\epsilon = W - W_a + h\nu$ is the excess energy of the electron over the maximum height of the potential barrier W_a of the emitting surface after receiving a quantum $h\nu$; $P(\nu, \epsilon)$ is the probability that an electron with energy W will absorb a quantum $h\nu$ and become a photo-electron; $D(\epsilon,E)$ is the probability that an electron with an energy ϵ will escape from the metal under the influence of an external electric field E. If one neglects photo-electric currents, which are generally orders of magnitude smaller than the currents of interest, (1) simplifies to

$$J \cong \int_{0}^{\infty} N(W)D(W,E)dW \qquad (2)$$

where $D(W,E)$ is the transmission probability that any of the N electrons from the Fermi energy distribution $N(W)$ with an energy W normal to the surface will escape from the metal under the influence of the applied electric field E. An approximate evaluation of (2) has been given for

the high temperature low field case by Dushman.[2]

Fowler and Nordheim[3,4] have treated the case for low temperature and high fields while Guth and Mullin[5] have extended these results to include the case for intermediate fields and temperatures.

For the case of interest here the field dependence of current density simplifies to

$$i = 1.55 \times 10^{-6} \frac{E^2}{\theta^2 \phi} \exp\left(-6.838 \times 10^7 \frac{\theta \phi^{3/2}}{E}\right) \text{ amp/cm}^2 \qquad (3)$$

where ϕ is the work function for a single crystal surface; θ is the Nordheim function of two elliptic integrals[4] and E is the externally applied field in volts/cm. Haefer[6] and more recently Dyke and Trolan[7] have checked this formula experimentally for very clean metals.

Because of the large size of very high voltage apparatus, metallic vacuum liners of the continuously evacuated type become a necessity. The vapor pressure of organic gasket materials usually limits the base pressure of such systems to the 10^{-5} or at best 10^{-6} mm Hg pressure range. In addition it is usually impractical and sometimes impossible to outgas large electrodes at high temperatures as in small x-ray tubes, etc.

Electron loading between unoutgassed metals in the pressure range of 10^{-4} to 10^{-8} mm Hg departs radically from the values predicted by the analytic given above.[8] In fact, electron loading is orders of magnitude larger and critical fields are much lower than predicted by (3). In addition large changes in electron loading result from contamination of the electrode with oil films.[9]

Because vacuum spark breakdown and electron loading represent basic limitations in the design of reliable vacuum insulated high voltage apparatus, care should be exercised in the selection of suitable electrode material. The results given below establish a basis for the selection of unoutgassed electride material in terms of relative electron loading and ability to hold high voltage in an organic-free mercury pumped system.

DESCRIPTION OF APPARATUS

Vacuum System

The all-metal vacuum system used for these experiments was continuously evacuated by a two-stage mercury diffusion pump. Interposed between the test cavity and the metal diffusion pump was a "multiple bounce" liquid nitrogen trap having a surface area of approximately two square feet. The high vacuum section of the system was built without a shut-off valve to eliminate the contamination of this section by organic vapors from the gasket material of a valve plate. A CO_2 trap isolated the mercury pump from the mechanical forevac pump. The general arrangement of the units is shown in Figure 1.

Cleaning of Vacuum System

All metal surfaces of the vacuum system were cleaned by sand blasting and prior to assembly were given a final wash in flowing C.P. acetone and C.P. ethyl alcohol. Insulators were scrubbed with scouring powder and rinsed with distilled water and acetone. Parts were assembled with clean cloth gloves and grease-free tools. All gaskets in the high vacuum section of the unit were made from 50 - 50 lead solder. Insulators were coupled to the system with lead foil (3 mil.) covered gum rubber gaskets.

Typical base pressures in this system were of the order of 10^{-7} mm Hg. The lowest recorded pressure on a liquid nitrogen trapped gauge was 8×10^{-8} mm Hg.

Electrodes

For the purpose of comparing metals, both gap electrodes were standardized to 1 inch radius hemispherically-capped cylinders. The electrode gap could be varied 1/2 inch while under vacuum load through a sylphon bellows at the metering (grounded) end of the cavity. Because of errors introduced by thermal expansion, the electrode gap was continuously monitored with a cathetometer.

High Voltage Supply

A 110 kv 10 ma supply having a ripple content of the order of 0.3 percent was used to charge the gap condenser. A voltage having a time constant of approximately 1/2 seconds was applied to the electrodes through a charging resistor which fed a .0125 μfd capacitor in parallel with the gap. (See Fig. 2).

EXPERIMENTAL TECHNIQUE

Determination of Electron Loading

Because electrode surfaces change radically with each spark, a different relation exists between electron loading and voltage after each breakdown. (See Fig. 3). In addition the current-voltage characteristics of the gap are quite dependent on the sparking history of the electrodes, the general trend being for decreased electron drain at a given voltage.

It has been found that for a given electrode material and a given parallel gap capacity, the drain voltage curves fall within reasonably well defined limits. Photographic monitoring was used in conjunction with the instrumentation shown in Fig. 2 to accumulate

sufficient statistical data on the current voltage characteristic of the electrode material in the gap. Multiple exposure photographs of this relation, as traced in linear coordinates on the face of an oscilloscope, were taken for several orders of magnitude of current. From an examination of a photograph of a hundred or more traces data were accumulated from which the upper and lower bounds of the junction could be obtained. The photographs for each metal were analyzed in terms of

$$I = BE^2 \exp(-b/E) \text{ amps} \qquad (4)$$

Values of B and b are reported for the extremes of the data so that definite bounds can now be placed on the relative electron loading of the materials listed below. It is, of course, impossible to give the specific electron loading of sparked electrode material under these test conditions because the microstructure of the surface, which is responsible for the current-voltage relation, cannot be determined.*

Effects due to variation in energy per spark, which are discussed below, were minimized in these tests by using the same parallel gap capacitor for all comparison tests. Unless prevented by power supply limitation, data were accumulated for a 0.2 mm electrode gap.

Spark Conditioning

Both breakdown voltage and voltage-current data are sensitive to the sparking history of the electrodes. Before reproducible data could be obtained it was necessary to spark the electrodes many thousand times. In general, electrode surfaces improve quite rapidly

---

* Even when the electrode surface is atomically smooth, single crystalline and of geometry known from electron photomicrographs, the best approximation of the surface field that can be made is still of the order of ± 15 percent. See Dyke and Trolan, loc. cit.

with the first few hundred sparks. For every metal tested except 316 stainless steel an equilibrium was reached within a few thousand sparks, see Fig. 4.

Breakdown Voltage Measurement

As may be noted from Fig. 5, it is impossible to define a unique breakdown voltage for any electrode material. One can, however, measure the frequency of breakdown as a function of voltage for a sufficient number of sparks and thereby determine a most probable breakdown voltage. If the voltage applied to electrodes continues to rise with time until a spark occurs, a skew distribution will be found, see Fig. 6, in the number of sparks which occur at each voltage. The breakdown voltage quoted below represents the voltage corresponding to the peak in such a curve.

Since a conditioning phenomena is associated with the number of sparks which occur, it is necessary to sample the breakdown voltage at several sparking intervals to determine whether or not an equilibrium has been reached. The relative values of breakdown voltages reported below represent the most probable breakdown voltage after this equilibrium has been reached.

RESULTS

Comparison of Metals by Electron Loading

Since the electrode spacing used was of the order of one percent of the radius of curvature of the electrodes, the gross surface gradient calculation was based on an infinite parallel-plane model.

Specific electron emission of the materials could not be measured in these experiments because of patch effect. That is, a major fraction of the electrons came from a few spots within an area of approximately one square centimeter in the high gradient region. If the data of Table I were to be used to estimate the electron emission from

electrodes of arbitrary shape a suitable summation process is indicated

$$I = B \sum_{o}^{n} A_i E_i e^{-b/Ei} \qquad (5)$$

were the total surface of interest divided into n parts each having a surface gradient E_i. The values of B and b are then assumed to apply for one square centimeter.

Even though the specific emission has not been determined, the use of identical electrodes and constant gap yields a good relative comparison of metals.

In the interpretation of the constant of Table I, which lists metals in the order of increasing electron loading, it should be understood that the term lower bound refers to the lowest current to be expected for a given gradient and vice versa.

Breakdown Voltage Scaling Relation

Although first published by Cranberg[10] it was discovered independently and almost simultaneously by R. L. Fortescue, Cranberg and Heard that a very simple relation exists between the most probable sparking voltage and the electrode spacing. Since that time much data for the d.c. case has been found to be in good agreement with the relation

$$VE = C \qquad (6)$$

where V is the total applied voltage E is the gross surface gradient and C is a number which depends on the electrode material and its surface treatment. For the parallel-plane case this relation reduces to (See Fig. 7)

$$V = kd\ 1/2 \qquad (7)$$

Comparison of Metals by Breakdown Voltage

Electrode materials are classified in this report in terms of

the coefficient k in (7) Table II lists the metals in the order of decreasing values of this coefficient. Test data are extrapolated to give this number for a 1 mm gap.

In comparing metals with respect to electron emission and breakdown voltage it will be noted that in general those metals which have a high breakdown voltage also have low electron emission. Specifically, however, the best materials for holding voltage do not yield the lowest electron emission.

DISCUSSION OF EXPERIMENTAL RESULTS

Effects of Gap Shunt Capacity

Current-Voltage Relation

A study was made of the effect of gap shunt capacity on the current-voltage relation. The gap shunt capacity was varied from 24×10^{-12} to 5×10^{-7} farads. A very pronounced and reproducible effect on the current-voltage characteristic was observed. (See Fig. 8). As will be noted from this photograph, the first spark at low capacity produces an immediate change in the electrode surface in a manner such as to increase the current drain at a given voltage. If the gap capacity is increased again, the current-voltage relation shows a definite "clean-up" to lower current at each voltage.

Quantitative data for these tests is shown in Fig. 9. These curves show that the primary variation is in the slope of the $\log_{10} (I/V^2)$ versus $1/V$ curve. This slope increases with decreasing field and increasing work function. One can argue that all sparks would produce about the same effect as far as the surface work function is concerned. It therefore appears that the more energetic sparks cause an increased radius of curvature at the cathode and thus decrease the local fields

to produce the observed results.

Electrode Surface Appearance

The surface appearance of electrodes was studied in an experiment where the gap shunt capacity was either 12.5×10^{-9} or 5×10^{-7} farads. A copper anode was placed opposite a manganese steel cathode so that good color contrast would be obtained for metal transferred to the cathode. The electrodes were observed after several sparks at 12.5×10^{-9} farads. A spray film of copper dust was found on the cathode. Some of this film had begun to peel up from the surface of the manganese steel cathode. The copper anode was covered with small pits of the order of 50 microns diameter. No evidence was found of any transfer of steel from the cathode.

A new pair of electrodes of identical construction was observed after several sparks with a parallel gap capacity of 5×10^{-7} farads. The surface of the manganese steel cathode showed evidence of surface melting. Ridges and wrinkles smoothered by surface tension were found on the surface. The direction of the smear metal ridges generally pointed away from the electrode center line. A very small amount of copper (d = 50 microns) was found on the steel cathode approximately 1 inch away from the electrode gap. This metal struck the surface as molten drops. The direction of the smear of the droplet indicated that the metal was moving away from the center line of the gap.

The observed difference in surface roughness was sufficient to cause the variation in electron drain with energy.

Breakdown Voltage-Gap Capacity Resonance

Measurements of the most probable breakdown voltage versus the parallel gap capacity were found to exhibit a resonance effect. Table III shows the most probable breakdown voltage versus parallel gap capacity.

Table III

Most Probable Breakdown Voltage Versus Parallel Gap Capacity

Invar Electrodes

Breakdown Voltage kv	Parallel Gap Capacity Micro farads
10	24×10^{-6}
60	12.5×10^{-3}
5	5×10^{-1}

Scatter in Current-Voltage Characteristics and Breakdown Voltage

Figure 10 illustrates the anomalous low voltage-high current trace which results when an incandescent spot appears on the anode prior to a spark.* In compiling the data for Table I such anomalous traces have been neglected.

Some statistics were accumulated on the location of the luminous spark discharge with respect to the minimum gap as correlated with the observed gap current and spark-over voltage. These data indicate that sparks which correspond to high current drains generally occur at other than the minimum gap. It appears slightly more probable that a spark will occur at the minimum gap if it occurs at a voltage at or above the most probable value. The scatter in voltage-current data is also associated with the dependence of the electron loading on the energy per spark. As illustrated in Figs. 5 and 6 the break-

* Inspection of one anode revealed a melted area in the location of this hot spot. Thus it appears that these areas are radiating due to incandescence as well as fluoresence.

down voltage and corresponding energy per spark will increase until a peak value is reached. The corresponding voltage-current data exhibit a similar "clean-up" phenomena. A spark at high voltage is usually followed by a distribution of low energy sparks and correspondingly high current drains at a given voltage.

Hardness Effect

A careful inspection of the class of metals with respect to breakdown voltage and electron loading reveals that the harder materials generally hold more voltage and exhibit lower current drains. To check this point for steel a set of electrodes was hardened to Rockwell C 60-65. These hardened electrodes held more voltage and had lower drain than found with ordinary hot-rolled steel. This is in agreement with the observation of Tonks[11] who found a marked increase in breakdown voltage when his mercury electrode was solidified by freezing.

Variation of Gap Current with Duty Cycle

The current-voltage characteristic for a 0.2 mm gap was studied when the sparking rate was changed from 35/min to 70/min. Fig. 11 shows that the gap current is higher before breakdown with increased duty factor. Within the accuracy of measurements with this technique there does not appear to be any change in the constants of equation (4) with duty cycle. The voltage and therefore the associated gap current occasionally appears to reach higher values with the increased duty cycle.

Comparison of Experimental Current-Voltage Data with Theory

Even though the experimental values of B in (4) exhibit considerable variation from metal to metal, values of B converge to a value which is several orders of magnitude smaller than is predicted by the Fowler-Nordheim field emission equation.[12] That is, experimental

values for B are of the order of 10^{-13} to 10^{-17} instead of 10^{-6} as predicted by the triangular potential barrier theory.

If the conventional values of the work functions for a pure metal lattice are used, the calculated emitting areas are 10^{-6} of the actual sparked area of the electrodes. The resultant current densities at these calculated emitting areas are of the order of 10^{5} to 10^{7} amp/cm^2, that is, order of the limiting current density to be expected for pure electron flow limited by space charge. For example, with 10^{5} volts applied to a 0.02 cm gap the maximum expected current density is of the order of 10^{5} amp/cm^2.

Further Observations of Patch Emission

Field emission microscope[13-15] observations were made of large cathodes (tip radius $\cong 10^{-3}$ cm) at pressures of the order of 10^{-5} mm Hg. The observed patterns on the fluorescent screen are in agreement with calculations which point to small patches as the predominant emitting areas on an electrode surface. Fig. 12 shows a typical photograph of one of several images which appear simultaneously on the fluorescent screen. Note in particular the bright crescent shaped areas.

It is not necessary to have extremely high gap gradients in order to observe these field emission patterns. Patches have been observed at gradients of the order of 10^{5} volts/cm and are commonly seen as bright patches on the anode electrode in the d.c. gap.

Effect of Surface Gradient at Constant Gap

Cathode gradient was varied in a fixed 15 cm gap by varying the radius of curvature of the electrodes. When the center electrode

of the spherically symmetric system had a radius of 0.5 cm, sparks could not be induced at 100 kv for either voltage polarity. No sparks occurred at 100 kv when the central electrode had a radius of curvature of 10^{-4} cm and was the anode. Rapid sparking resulted when the high gradient electrode became the cathode. This continued until sparking increased the radius of curvature of the cathode to approximately 1/64 inch. Luminous vapor was observed to project 6 - 8 cm out from the cathode during spark erosion.

These results demonstrate that cathode surfaced gradient and total voltage rather than electrode spacing are important in determining breakdown voltage for a given gap. That is, the observed square-root dependence between voltage and sparking is only correct for parallel plane geometry.

Breakdown Voltage Distribution

When the breakdown voltage of a given material is measured with a slowly rising applied voltage, a skew distribution exists between the sparking probability and voltage. (See Fig. 6).

Statistically, the existence of a skew rather than a Gaussian distribution can be interpreted as relating sparking pheonomena to one or at most a very few dominant events. While this very general piece of information does not define the spark mechanism it does show that the phenomena is not extremely complicated and in fact may be capable of explanation by a single process. A simple process such as recently described by Cranberg[16] may very well be the correct interpretation of vacuum sparking.

Effects of Using Dissimilar Electrode Materials

An experiment was performed to determine which electrode

predominates in determining the breakdown voltage in a vacuum gap. The electrodes were geometrically identical. An Inconel anode (the high voltage electrode) was placed opposite a carbon (C-15) cathode and vice versa. These combinations are compared with an all carbon and an all Inconel gap in the Table IV.

Table IV

Permutations of Carbon and Inconel as Electrodes

Cathode	Anode	Most Probable Breakdown Voltage for 1 mm gap
Inconel	Carbon	48 kv
Carbon	Carbon	52 kv
Carbon	Inconel	62 kv
Inconel	Inconel	134 kv

These results show that for a symmetrical gap the anode material plays a predominant role in determining the breakdown voltage. Continued sparking caused the most probable sparking voltage to be lowered from 48 to 44 kv for the Inconel cathode-carbon anode combination. Inspection of electrodes on removal revealed loose carbon flakes which had begun to peel from the Inconel cathode. Similarly, the breakdown voltage for the carbon cathode-Inconel anode combination eventually dropped to 30 kv at which time Inconel spray metal was obviously beginning to peel from the cathode.

If the gap contains dissimilar metals, the breakdown voltage will be lower than that of the best electrode material. Where extreme differences exist in the physical properties of the cathode-anode metals the breakdown voltage of the gap may be lower than that of the poorest electrode material used.

CONCLUSIONS

1. Sparking is cathode gradient dependent. Design of high voltage cathodes electrodes should incorporate the maximum practical radius of curvature.

2. By proper choice of electrode materials a maximum gain of approximately seven in voltage holding may be obtained.

3. Breakdown voltage for parallel-plane d-c gaps scales approximately as the square-root of the electrode spacing.

4. The stored energy which can be discharged into a vacuum spark has a pronounced effect on the electrode drain and breakdown voltage. Sparks at low stored energy produce finely divided spray metal which causes a large increase in electron loading.

5. High vacuum sparking depends upon a statistical event. Much data is required before a good estimate of the most probable breakdown voltage can be obtained.

6. Most of the electron loading comes from microscopic patches on the electrodes.

7. Statistical data can be accumulated which will predict the bounds of the electron loading for a given electrode material even though the metal is not outgassed and is operated at pressures in the 10^{-6} to 10^{-8} mm Hg range. These data are sensitive to the energy discharged in the vacuum spark.

8. The best materials tested for holding high voltages are the steels and nickel-steel alloys.

9. Hardening an electrode material increases its ability to hold voltage and reduces the electron loading.

10. Electron loading of unoutgassed materials varies exponentially with electric field.

11. Cathode and anode electrodes should be fabricated from the same material.

12. Statistical data show that there is one or at most only a very few events which are dominant in the initiation of the d-c vacuum spark.

ACKNOWLEDGMENTS

The author is indebted to Dr. E. J. Lofgren for his valuable suggestions and criticisms during the course of this work.

Other persons who assisted in measurements and services include: Paul Byerly, R. Carpenter, J. DePue, N. Fletcher, M. Jones, E. Lauer, Robert Richter and Howard Smith.

REFERENCES

1. E. Guth and C. Mullen, Phys. Rev., 59, 867 (1941)
2. S. Dushman, Rev. Mod. Phys., 2, 381 (1930)
3. R. H. Fowler and L. W. Nordheim, Proc. Roy. Soc., 119, 173 (1928)
4. L. W. Nordheim, Proc. Roy. Soc., 121:A, 626 (1928)
5. E. Guth and C. J. Mullen, Phys. Rev., 59, 575 (1941); 61, 339 (1942)
6. R. Haefer, Zeit f. Phys., 116, 604 (1940)
7. W. P. Dyke and J. K. Trolan, Phys. Rev., 89, 799 (1953)
8. Penning and Mulder, Physics, 2, 724 (1935)
9. R. L. Steward, Phys. Rev., 45, 499 (1934)
10. L. Cranberg, J.A.P., 23, 518 (1952)
11. L. Tonks, Phys. Rev., 48, 562 (1935)
12. A. Sommerfeld and H. Bethe, Handbuch der Physik,(1934) 24, Pt. 2, Sec. 3 Art. 19, -. 436
13. R. P. Johnson and W. Schockley, Phys. Rev., 49, 436 (1936)
14. E. W. Muller, Zeit f. Physik, 108, 668 (1938)
15. E. W. Muller, Naturwissenschaften, 37, 333 (1950)
16. Cranberg, loc. cit.

TABLE I

FIELD EMISSION CONSTANTS FOR SPARK CONDITIONED OUTGASSED METALS IN A MERCURY PUMPED HIGH VACUUM CAVITY

$I = BE^2 e^{-b/E}$ I = amps, E = volts/cm

Electrode Material	Upper Bound		Lower Bound		Data After N-Sparks
	$10^{-5} \times b$	$10^{17} \times B$	$10^{-5} \times b$	$10^{17} \times B$	
Case Hardened Steel	444	141	58.2	8.7	24,000
316 Stainless Steel	436	31,600	51.7	4.37	60,000
General Plating Alloy No. 720	340	10,200	46.1	10.7	15,000
Hastalloy B	303	224	34.6	31.6	13,000
32% Ni Steel	278	6,450	161	148	10,000
Invar	272	135	91.5	67.6	26,000
Inconel	179	2,040	32.6	64.6	12,000
Tantalum	176	1,990	10.6	5.88	15,000
C-15 Anodic Carbon	171	251,000	63.8	132	2,500
Chromium Plated Copper (.001 in)	169	358	50.4	282	12,500
Spectrographic Carbon	158	79,500	21.0	70.8	10,000
Hot Rolled Steel	145	19,100	69.8	309	85,000
Manganese Steel	134	50	105	20.9	27,000
E.T.P. Copper	131	814,000	12.0	3,540	10,800
Nickel	122	4,580	11.1	365	13,000
Vacuum Fused Copper	93.8	24,000	----	---	24,000
Cupalloy	76.3	50,200	28.2	7,080	11,000
2-S Aluminum	38.2	2,510	3.12	49.0	9,000
Silver	29.4	63,100	3.07	4,170	25,000
Tungsten	----	-----	40.4	13,500	9,100
Molybdenum	----	-----	28.1	1,380	43,000
75-ST-6 Aluminum	7.83	4,680	5.93	3,460	20,000

TABLE II

BREAKDOWN COEFFICIENTS FOR SPARK CONDITIONED UNOUTGASSED METALS IN A MERCURY PUMPED HIGH VACUUM CAVITY

$$V = kd^{\frac{1}{2}}$$

ELECTRODE MATERIAL	BREAKDOWN COEFFICIENT (KILOVOLTS/$(mm)^{\frac{1}{2}}$)	DATA AFTER N-SPARKS
Invar	197	25,000
316 Stainless Steel	179	56,000
Manganese Steel	172	27,000
General Plating - Alloy No. 720	161	19,000
Case Harden Steel (Rc=60-65)	159	12,500
Chrome Plated Copper (.001 in) 500° C Bake	143	5,000
Inconel	134	12,000
32% Ni Steel	134	20,000
Hastalloy B	126	25,000
Nickel	89.5	13,000
Chrome Plated Copper (.001 in) No Bake	89.4	40,000
Hot-Rolled Steel	89	62,400
E.T.P. Copper	74	22,500
Cupalloy	71	11,000
Tantalum	71	20,000
Aluminum (2S)	57	8,700
Lead	54	12,500
Vacuum Fused Copper	54	24,000
75 ST-6 Aluminum	45	20,000
C-15 Anodic Carbon	36	10,000
Spectrographic Carbon	36	14,000
Silver	27	14,000

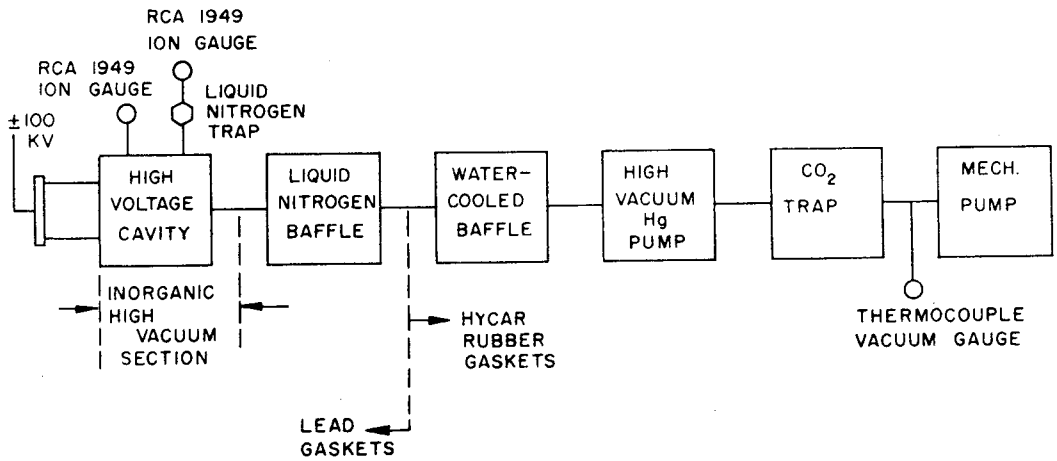

HIGH VACUUM TEST CAVITY

FIG. 1

MU-5851

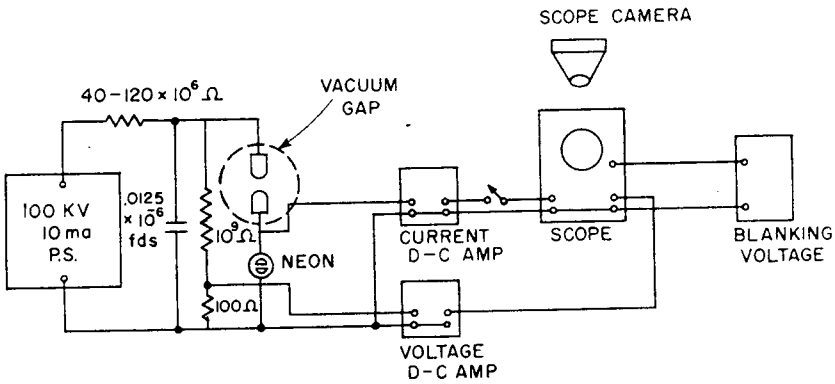

INSTRUMENT ARRANGEMENT

FIG. 2

MU-5852

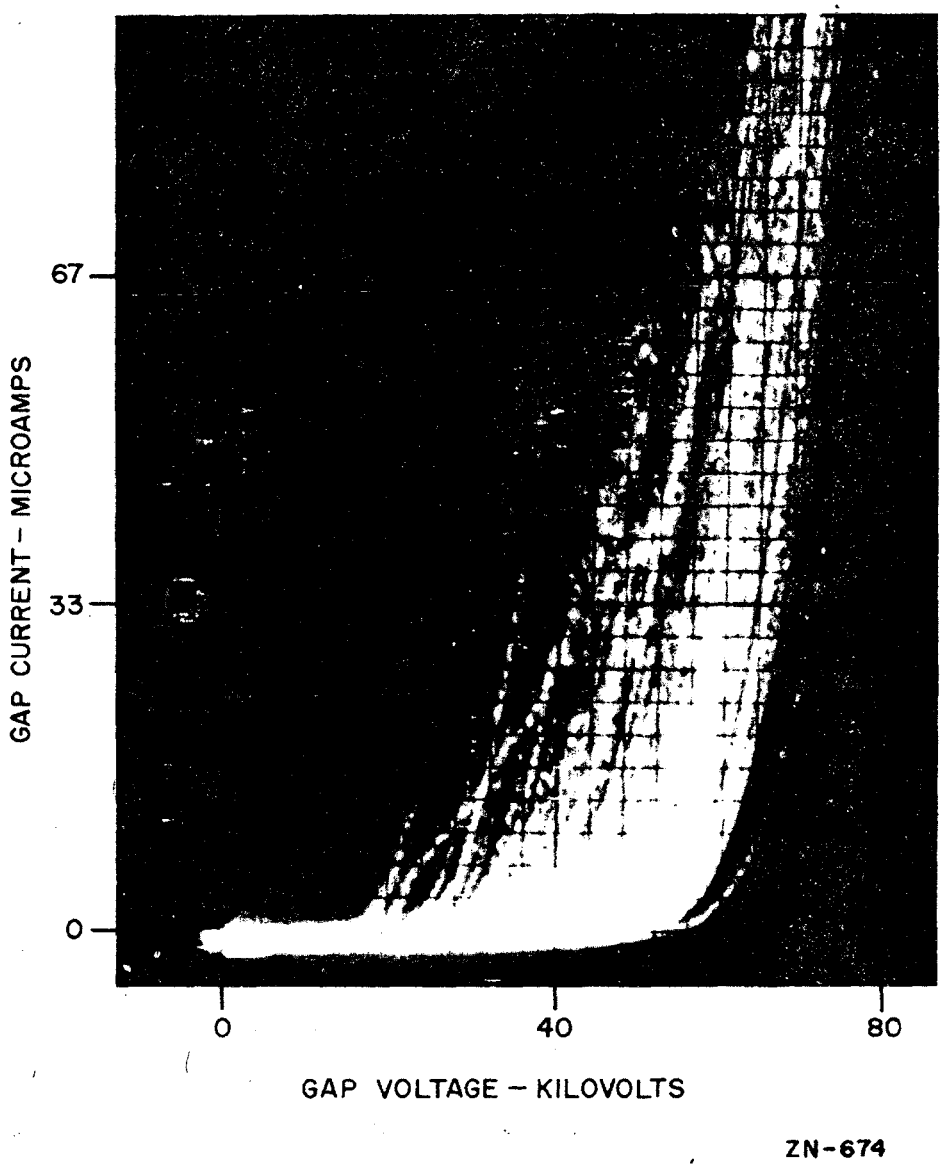

Fig. 3. Typical scatter of voltage-current data. 316 stainless steel electrodes after 50,000 sparks at 10 to 50 joules per spark. Electrode spacing 0.2 $\pm$ .05 mm.

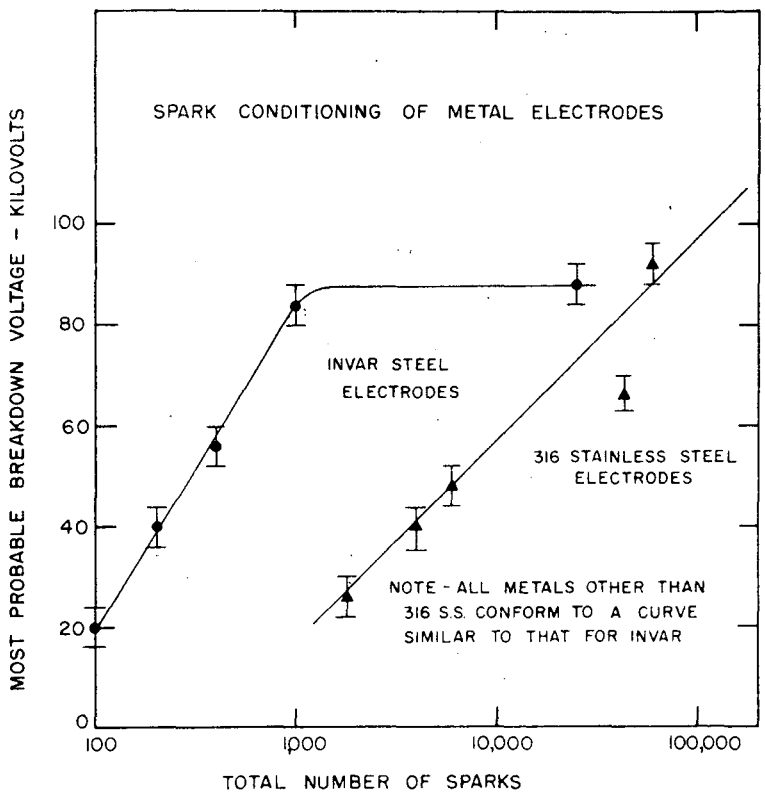

VARIATION OF MOST PROBABLE BREAKDOWN VOLTAGE WITH NUMBER OF SPARKS

FIG. 4

MU-5853

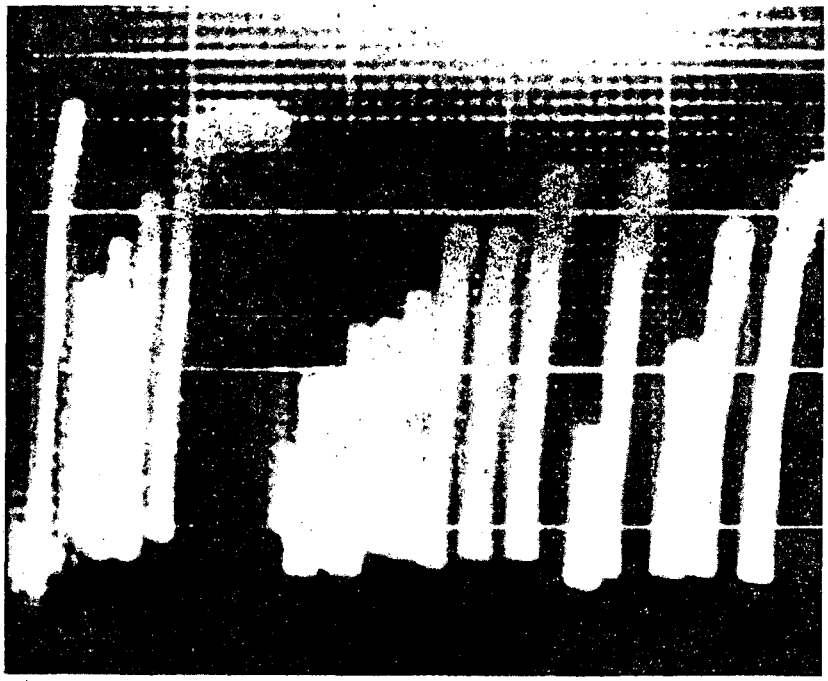

RELATIVE TIME ⟶

ZN-675

Fig. 5 Variation of breakdown voltage for a constant gap. Note in particular that a spark at high voltage is usually followed by a flurry of sparks at lower voltages. Note also the clean-up of sparking to higher voltages. This behavior is characteristic of all vacuum sparks where sufficient voltage can be applied to cause gap breakdown.

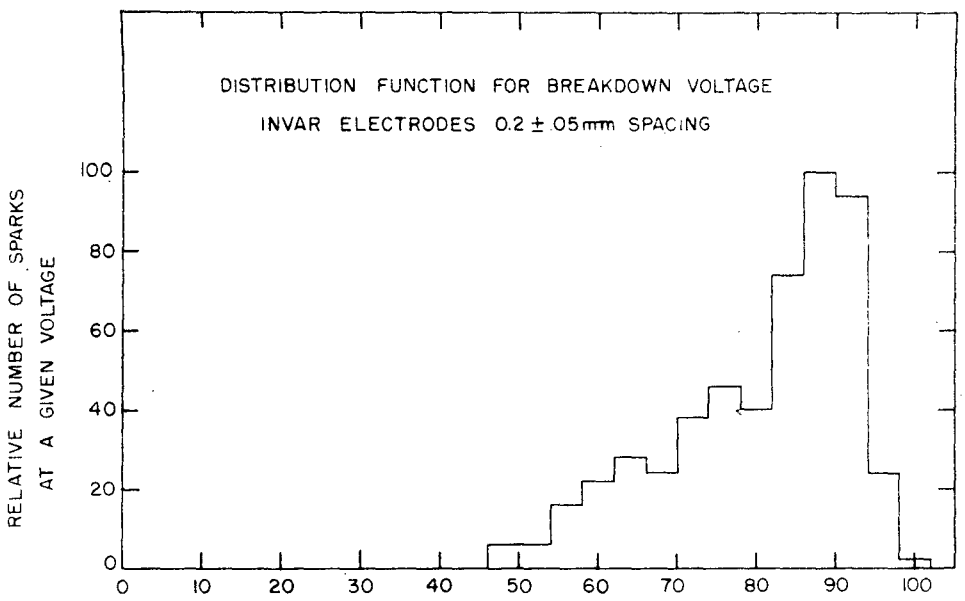

BREAKDOWN VOLTAGE DISTRIBUTION

FIG. 6

MU-5854

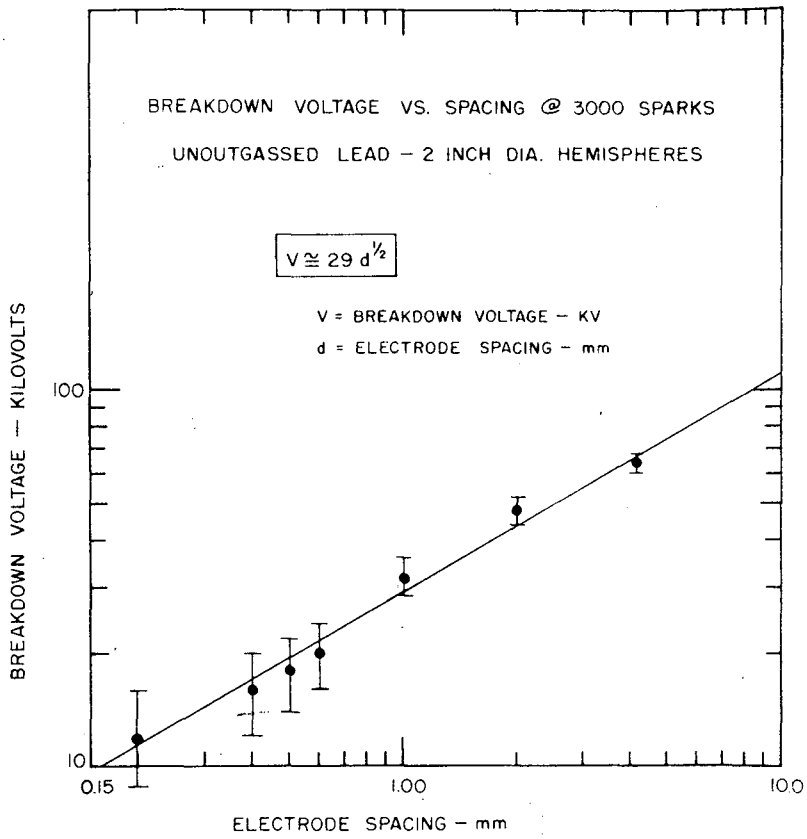

VARIATION OF BREAKDOWN VOLTAGE WITH ELECTRODE SPACING

FIG. 7

MU-5855

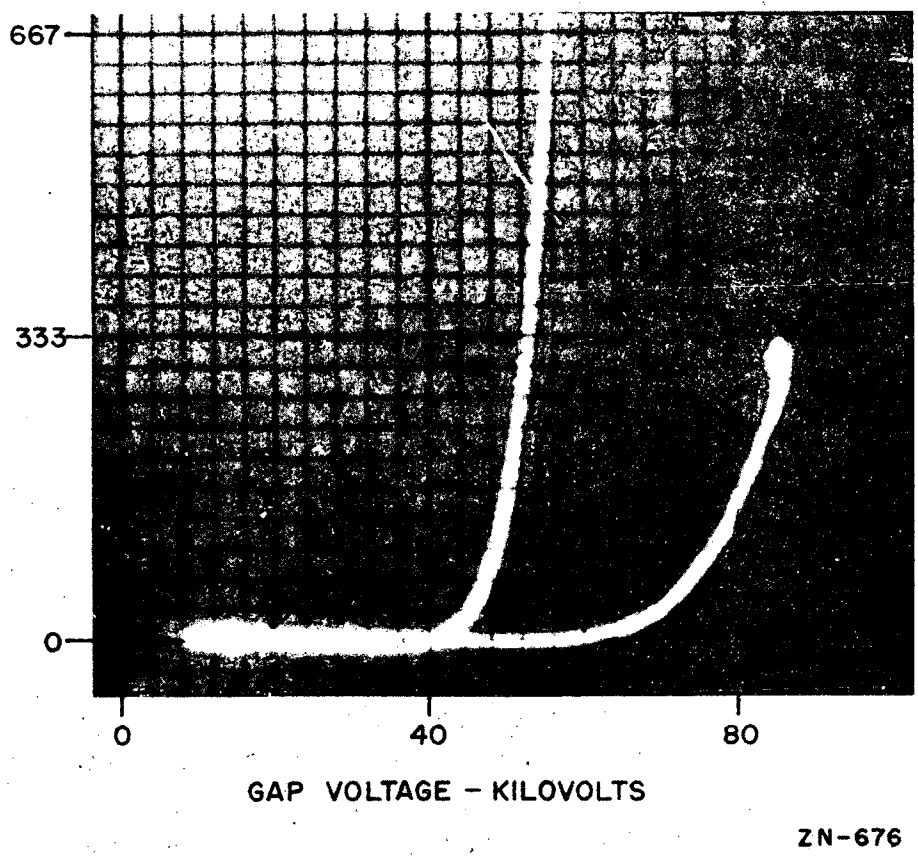

Fig. 8. Increase in gap current following a low energy spark. Sequence: (1) Spark electrodes many times with parallel gap capacity of 833 x 10^{-12} farads. Change gap capacity to 118 x 10^{-12} farads. (2) Photograph the current-voltage characteristics of the next two sparks. The low current high voltage curve represents the surface just prior to the first low energy spark.

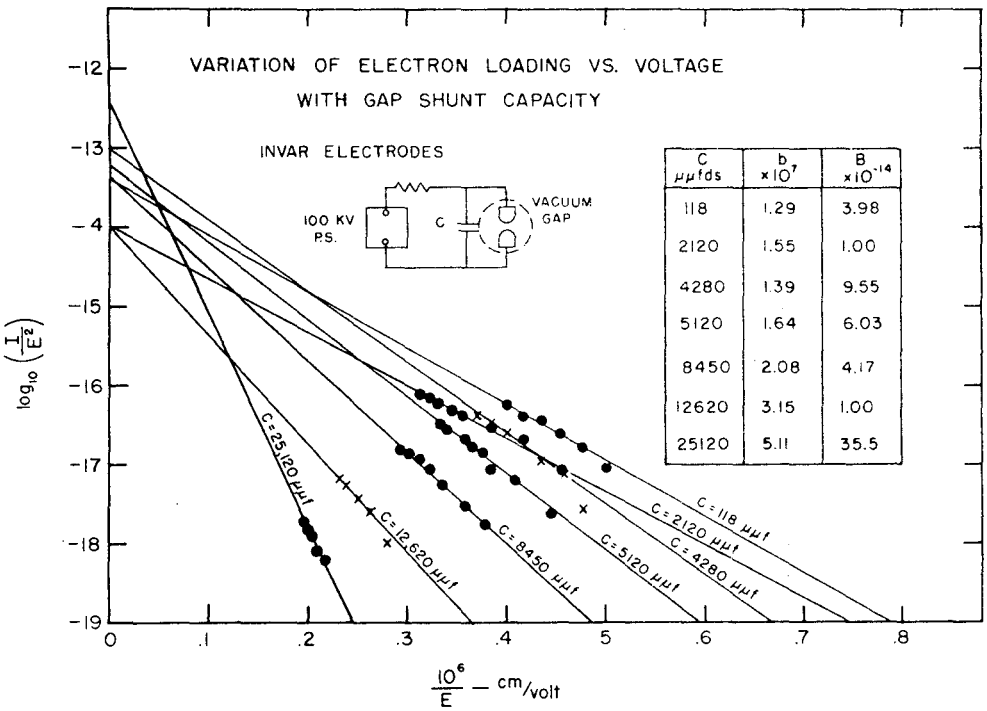

EFFECT OF ENERGY PER SPARK ON VOLTAGE – CURRENT RELATION

FIG. 9

MU-5856

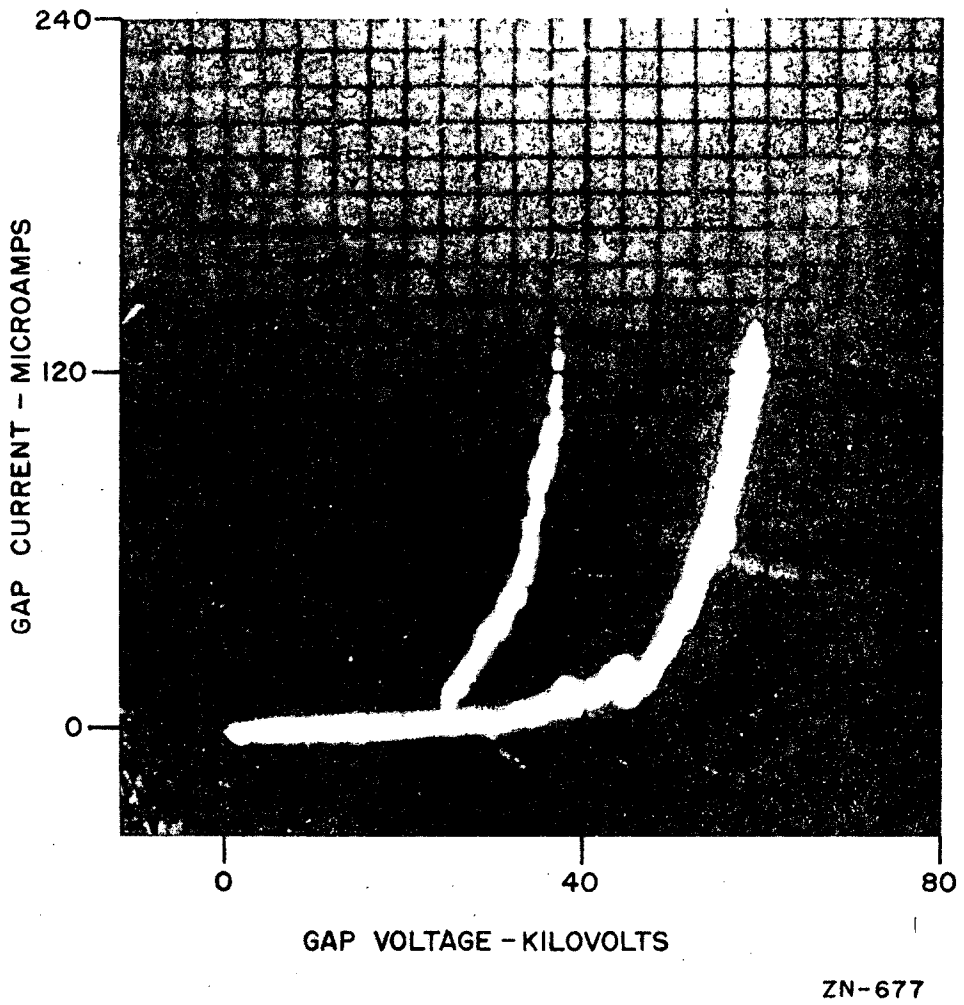

Fig. 10. Anomolous current-voltage data. The jagged structure of the low voltage high current pre-spark drain correlates with the appearance of an incandescent spot on the anode surface.

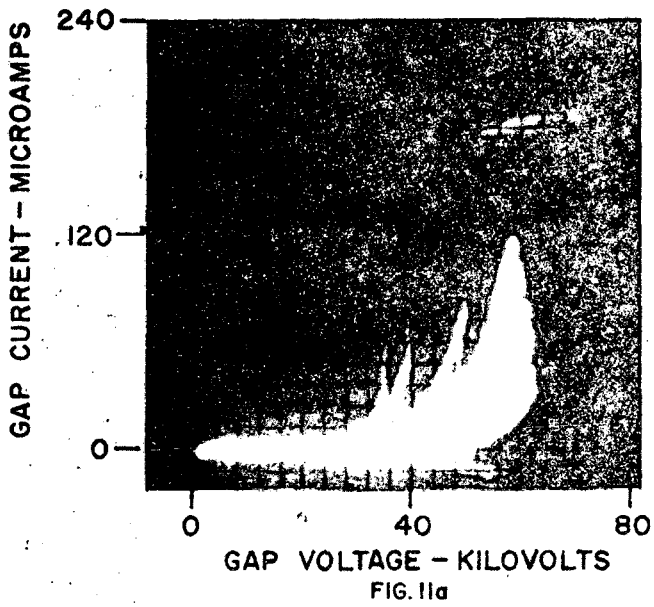

FIG. IIa

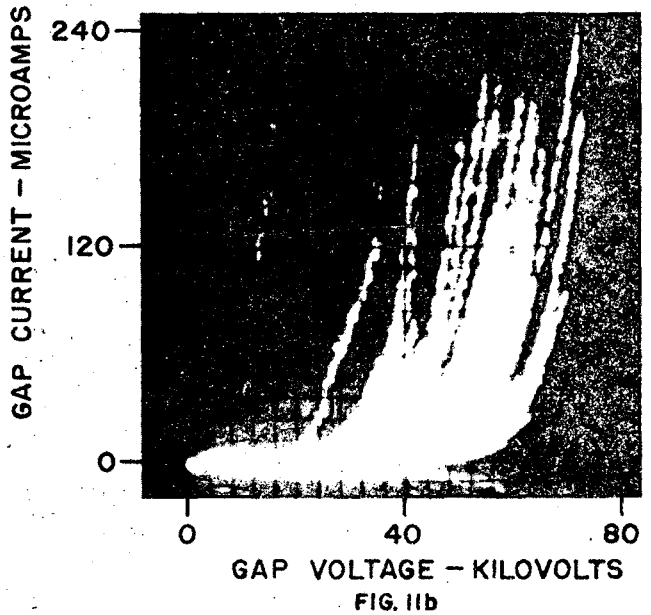

FIG. IIb

Fig. 11 Current-voltage relations for 32% nickel steel.

(a) Sparking rate 35/minute

(b) Sparking rate 70/minute

ZN-679

Fig. 12. Typical field emission pattern from large copper cathode in vacuum of the order of 10^{-5} mm Hg. Note the two crescent shaped bright patches near the large emitting area.